

RESEARCH

Open Access



Posterior fossa ependymoma H3 K27-mutant: an integrated radiological and histomolecular tumor analysis

Cassandra Mariet¹, David Castel², Jacques Grill^{1,2}, Raphaël Saffroy³, Volodia Dangouloff-Ros^{4,5}, Nathalie Boddaert^{4,5}, Francisco Llamas-Gutierrez⁶, Céline Chappé⁷, Stéphanie Puget⁸, Lauren Hasty⁹, Fabrice Chrétien⁹, Alice Métais^{9,10}, Pascale Varlet^{9,10} and Arnault Tauziède-Espariat^{9,10*}

Abstract

Posterior fossa group A ependymomas (EPN_PFA) are characterized by a loss of H3 K27 trimethylation due to either *EZH1P* overexpression or H3 p.K27M mutation, similar to H3 K27-altered diffuse midline gliomas (DMG), but in reverse proportions. Very little data is available in the literature concerning H3 K27M-mutant EPN_PFA. Here, we retrospectively studied a series of nine pediatric tumors initially diagnosed as H3 K27M-mutant EPN_PFA to compare them to *EZH1P*-overexpressing EPN_PFA in terms of radiology, follow-up, histopathology, and molecular biology (including DNA-methylation profiling). Seven tumors clustered within EPN_PFA by DNA-methylation analysis and t-distributed stochastic neighbor embedding. Among the two remaining cases, one was reclassified as a DMG and the last was unclassified. H3 K27M-mutant EPN_PFA cases were significantly older than their counterparts with an *EZH1P* overexpression. Radiological and histopathological central review of our seven H3 K27M-mutant EPN_PFA cases found them to be similar to their counterparts with an *EZH1P* overexpression. Sequencing analyses revealed *HIST1H3B* (n = 2), *HIST1H3C* (n = 2), *H3F3A* (n = 1), and *HIST1H3D* (n = 1) K27M mutations (no sequencing analysis available for the last case which was immunopositive for H3K27M). Consequently, *HIST1H3C/D* mutations are more frequently observed in EPN_PFA than in classic pontine DMG, H3K27-mutant. Overall survival and event-free survival of *EZH1P*-overexpressing and H3 K27M-mutant EPN_PFA were similar. After surgery and radiation therapy, 5/7 patients were alive at the end of the follow-up. In summary, the diagnosis of EPN_PFA must include tumor location, growth pattern, Olig2 expression, and DNA-methylation profiling before it can be differentiated from DMG, H3 K27-altered.

Keywords: Posterior fossa, Ependymoma, Histones, DNA-methylation

Introduction

In the central nervous system (CNS), the loss of H3 p.K27me3 expression generally constitutes the hallmark of two different tumor types: diffuse midline glioma (DMG), H3 K27-altered and posterior fossa ependymoma, subtype A (EPN_PFA) [6, 15]. This loss is

due to an overexpression of *EZH1P* or to K27M mutations in histone H3 genes (mostly *H3F3A* and *HIST1H3B*), inhibiting the methyltransferase activity of the Polycomb Repressive Complex 2 (PRC2) [5]. *EZH1P* overexpression and H3 K27M mutations are mutually exclusive and are encountered in reverse proportions: 3% versus 97% and 96% versus 4%, respectively in DMG and EPN [15]. K27M histones' genes mutations have also been exceptionally reported in other tumor types, such as one desmoplastic/nodular medulloblastoma, SHH-activated [7], one embryonal tumor with multilayered rosettes of

*Correspondence: a.tauziède-espariat@ghu-paris.fr

⁹ Department of Neuropathology, GHU Paris-Psychiatrie Et Neurosciences, Sainte-Anne Hospital, 1, rue Cabanis, 75014 Paris, France
Full list of author information is available at the end of the article



© The Author(s) 2022. **Open Access** This article is licensed under a Creative Commons Attribution 4.0 International License, which permits use, sharing, adaptation, distribution and reproduction in any medium or format, as long as you give appropriate credit to the original author(s) and the source, provide a link to the Creative Commons licence, and indicate if changes were made. The images or other third party material in this article are included in the article's Creative Commons licence, unless indicated otherwise in a credit line to the material. If material is not included in the article's Creative Commons licence and your intended use is not permitted by statutory regulation or exceeds the permitted use, you will need to obtain permission directly from the copyright holder. To view a copy of this licence, visit <http://creativecommons.org/licenses/by/4.0/>. The Creative Commons Public Domain Dedication waiver (<http://creativecommons.org/publicdomain/zero/1.0/>) applies to the data made available in this article, unless otherwise stated in a credit line to the data.

the posterior fossa (harboring also a *DICER1* mutation) [20], and *BRAF*-mutant midline gangliogliomas [9, 10, 14]. Because of these potential histomolecular diagnostic pitfalls, the Consortium to Inform Molecular and Practical Approaches to CNS Tumor Taxonomy—Not Official WHO (cIMPACT-NOW), and the World Health Organization (WHO) classification of tumors of the CNS clarified the definition of the DMG, H3 K27-altered, in which each term is mandatory: diffuse (infiltrating the neuropil background, particularly on neurofilament staining), midline (including thalamus, brainstem and spinal cord), and glioma (with the expression of glial markers, particularly Olig2) [11, 12]. Thus, a tumor previously initially diagnosed as a brainstem DMG, EZHIP-overexpressing, was reclassified as an EPN_PFA by DNA-methylation analysis [16]. Interestingly, this tumor met two of the three essential DMG diagnostic criteria (midline location and infiltrative, but did not express Olig2) [16]. DMG may present a wide variety of morphologies including ependymoma-like features [3, 12, 18]. Very few histopathological and epigenetic data are available for previously described EPN_PFA with H3 K27M mutation (22 published cases) [8, 13, 15, 17, 21]. To explore this issue, we investigated a cohort of 147 EPN_PF to detect H3 K27M-mutant cases in order to better characterize them in terms of radiology, follow-up, histopathology, and molecular biology (including DNA sequencing and DNA-methylation profiling).

Methods

Sample collection

Tumor samples of EPN_PF were provided by the consultation archive database (1993–2021) from the department of neuropathology at GHU-Paris Psychiatry and Neurosciences, Sainte-Anne Hospital. Thereafter, we screened the national French neuropathological network database and searched for other cases presenting the same histopathology.

This study was approved by our local ethics committee. Written informed consent for clinical and imaging investigations and molecular analysis was obtained from all patients enrolled in this study.

Clinical and radiological data

Patient characteristics and clinical data retrieved from hospital records included: sex, age at presentation, and medical history. The central radiological review of pre-operative magnetic resonance imaging (MRI) was performed by two senior neuroradiologists (VDR and NB). The following features were evaluated: location (tumor epicenter), size, volume, signal in T1-weighted sequence, T2-weighted sequence, susceptibility imaging, diffusion and apparent coefficient diffusion map (ADC), contrast

enhancement, contours, presence of cysts, necrosis, and perfusion parameters.

Central histopathological review and immunohistochemistry

The central pathology review was performed conjointly by two neuropathologists (ATE and PV). According to the last WHO classification, no grading was applied. A representative paraffin block was selected for each case. Unstained 3- μ m-thick slides of formalin-fixed, paraffin-embedded tissues were obtained and submitted for immunostaining. The following primary antibodies were used: Glial Fibrillary Acidic Protein (GFAP) (1:200, clone 6F2, Dako, Glostrup, Denmark), epithelial membrane antigen (1:200, clone GM008, Dako, Glostrup, Denmark), Olig2 (1:3000, clone C-17, Santa Cruz Biotechnology, Dallas, USA), Neurofilament Protein (1:100, clone 2F 11, Dako, Glostrup, Denmark), H3K27me3 (1:2500, polyclonal, Diagenode, Liege, Belgium), EZHIP (1:75, polyclonal, Sigma-Aldrich, Bromma, Sweden) and H3K27M (1:5000, clone EPR18340, Abcam, Cambridge, United Kingdom). External positive and negative controls were used for all antibodies.

Detection of H3 K27M mutation by MassArray and Sanger Sequencing

Genomic DNA was extracted from formalin-fixed and paraffin-embedded (FFPE) tissue. K27M mutations in *H3F3A*, *HIST1H3B* and *HIST1H3C* were detected using the Massarray iPLEX technology (Agena Bioscience). The Massarray iPLEX procedure involves a three-step process consisting of the initial PCR reaction, inactivation of unincorporated nucleotides by shrimp alkaline phosphatase and a single-base primer extension. The products are then nano-dispensed onto a matrix-loaded silicon chip (SpectroChipII, Agena Bioscience) and finally, the mutations are detected by MALDI–TOF (matrix-assisted laser desorption-ionization–time of flight) mass spectrometry. Data analysis was performed using MassArrayTyper Analyzer software 4.0.4.20 (Agena Bioscience). Negative cases with sufficient gDNA were further submitted for a whole exome analysis (WES) at Integragen (Evry, France) and analysed as previously published [5]. When this technique was not contributive, genomic DNA was extracted from fresh-frozen or formalin-fixed and paraffin-embedded (FFPE) tissue. K27M mutations in *H3F3A*, *HIST1H3B* and *HIST1H3C* were detected by direct Sanger sequencing of PCR amplified products from tumor genomic DNA as previously published [6]. Negative cases with sufficient gDNA were further submitted to a whole exome analysis (WES) at Integragen (Evry, France) and analysed as previously published [5].

DNA methylation array processing and copy number profiling

DNA extraction from FFPE was performed using the QIAamp DNA FFPE Tissue Kit and the Qiacube (QIAGEN, Hilden, Germany) according to the manufacturer's instructions. 250 to 500 ng of DNA were extracted from each tissue sample. Kits used for bisulfite conversion and reparation were the Zymo EZ DNA methylation kit and ZR-96 DNA Clean and Concentrator-5 (Zymo Research, Irvine, CA) and bisulfite DNA was processed using the Illumina Infinium HD FFPE DNA Restore kit and Infinium FFPE QC kit (Illumina, San Diego, CA). The DNA was then processed using the Illumina Infinium Human-Methylation EPIC Bead-Chip array (Illumina, San Diego, CA) according to the manufacturer's instructions. The iScan control software was used to generate raw data files from the BeadChip in IDAT format and analyzed using GenomeStudio version 2.0 (Illumina, San Diego, CA). The following filtering criteria were applied: removal of probes targeting the X and Y chromosomes, removal of probes containing single nucleotide polymorphisms (dbSNP132 Common) within five base pairs of and including the targeted CpG site, and removal of probes not mapping uniquely to the human reference genome (hg19), allowing for one mismatch [4]. The raw IDAT files were uploaded to www.molecularneuropathology.org for supervised analysis using the Random Forest methylation class prediction algorithm, as previously described [4]. All computational analyses were performed in R version 3.3.1 (R Development Core Team, 2016; <https://www.R-project.org>). Copy-number variation analyses from 450 k and EPIC methylation array data were performed using the *conumee* Bioconductor package version 1.12.0. Raw signal intensities were obtained from IDAT-files using the *minfi* Bioconductor package version 1.21.4. Illumina EPIC samples and 450 k samples were merged to a combined data set by selecting the intersection of probes present on both arrays (*combineArrays* function, *minfi*). Each sample was individually normalized by performing a background correction (shifting of the 5% percentile of negative control probe intensities to 0) and a dye-bias correction (scaling of the mean of normalization control probe intensities to 10,000) for both color channels. Subsequently, a correction for the type of material tissue (FFPE/frozen) and array type (450 k/EPIC) was performed by fitting univariable, linear models to the log₂-transformed intensity values (*removeBatchEffect* function, *limma* package version 3.30.11). The methylated and unmethylated signals were corrected individually. Beta-values were calculated from the retransformed intensities using an offset of 100 (as recommended by Illumina). All samples were checked for duplicates by pairwise correlation of the genotyping

probes on the 450 k/850 k array. To perform unsupervised non-linear dimension reduction, the remaining probes after standard filtering were used to calculate the 1-variance weighted Pearson correlation between samples. The resulting distance matrix was used as input for t-SNE analysis (t-distributed stochastic neighbor embedding; *Rtsne* package version 0.13). The following non-default parameters were applied: $\theta = 0$, $pca = F$, $max_iter = 20,000$ $perplexity = 10$. The t-SNE analysis was performed and compared with the genome-wide DNA methylation profiles from selected reference groups of the brain tumor reference cohort [4].

Results

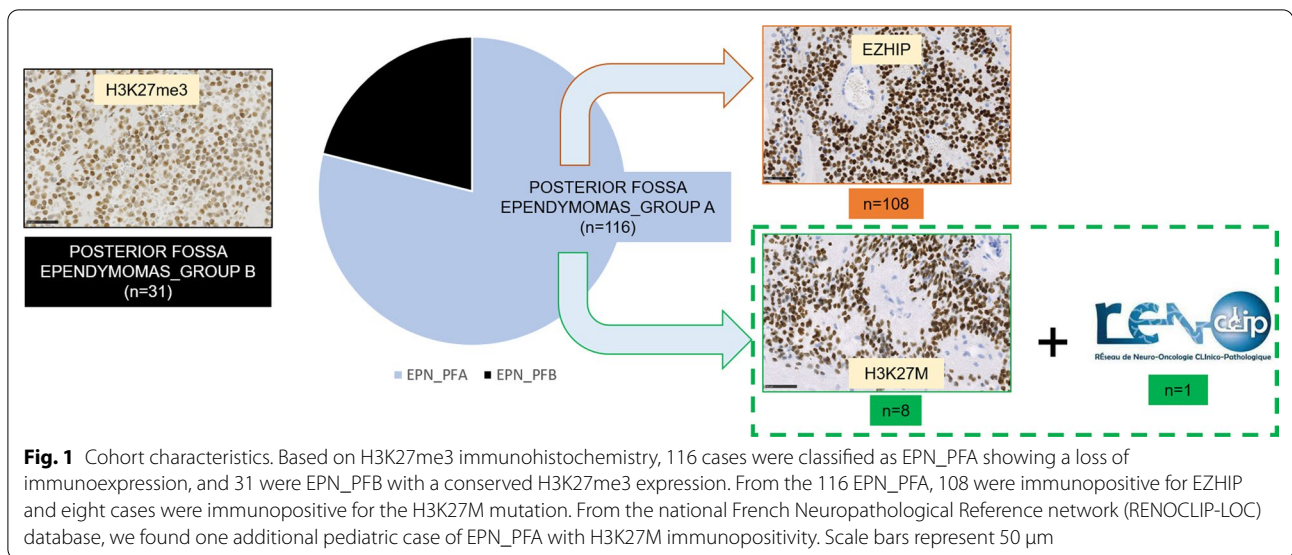
Of the 147 tumors classified as EPN_PF, 5% of them exhibited a H3 K27M immunopositivity

147 cases were retrieved and reviewed by two pathologists (PV and ATE). 131 (89%) patients were children and 16 (11%) were adults. The median age of the whole cohort was 8-years-old (aged from 0 to 72-years-old). The female to male ratio was 0.9 (71 females and 76 males). Based on immunohistochemistry, 116 cases were EPN_PFA (all pediatrics) showing a loss of H3K27me₃ immunopositivity, and 31 were EPN_PFB (15 children and 16 adults) with a conserved H3K27me₃ expression. From the 116 EPN_PFA, 108 (93%) were immunopositive for EZHIP and eight cases (7%, 5% of the whole cohort) were immunopositive for the H3K27M mutation. From the national French Neuropathological Reference network (RENOCLIP-LOC) database, we found one additional pediatric case of EPN_PFA with H3K27M immunopositivity (Fig. 1).

Posterior fossa tumors with ependymal/subependymal features, H3 K27M-positive encompass different subgroups with distinct clinical outcomes

We subjected these nine H3 K27M EPN_PFA cases to DNA-methylation profiling (with the v12.5 of the DKZF classifier of CNS tumors), and 5/9 cases presented a high calibrated score (≥ 0.9), classified as EPN_PFA, subclass 1f (#1, 2, 4, 5, and 7). We also performed a t-SNE analysis on the nine cases to better classify tumors with low calibrated scores (< 0.9) (Fig. 2) and integrate it with clinical, radiological and histomolecular findings.

Accordingly, six cases (#1, 2, 3, 4, 5 and 7) were classified by DNA-methylation profiling as EPN_PFA (Fig. 2, Additional file 1: Supplementary Fig. 1 for copy number variations). They were located in the fourth ventricle. All but one had a K27M mutation of one of the genes encoding for the H3.1 protein (*HIST1H3B* in two cases, *HIST1H3C* in two cases, and *HIST1H3D* in one case). For the last case (#2), DNA sequencing analyses failed to reveal any mutation of histones' genes due to the poor



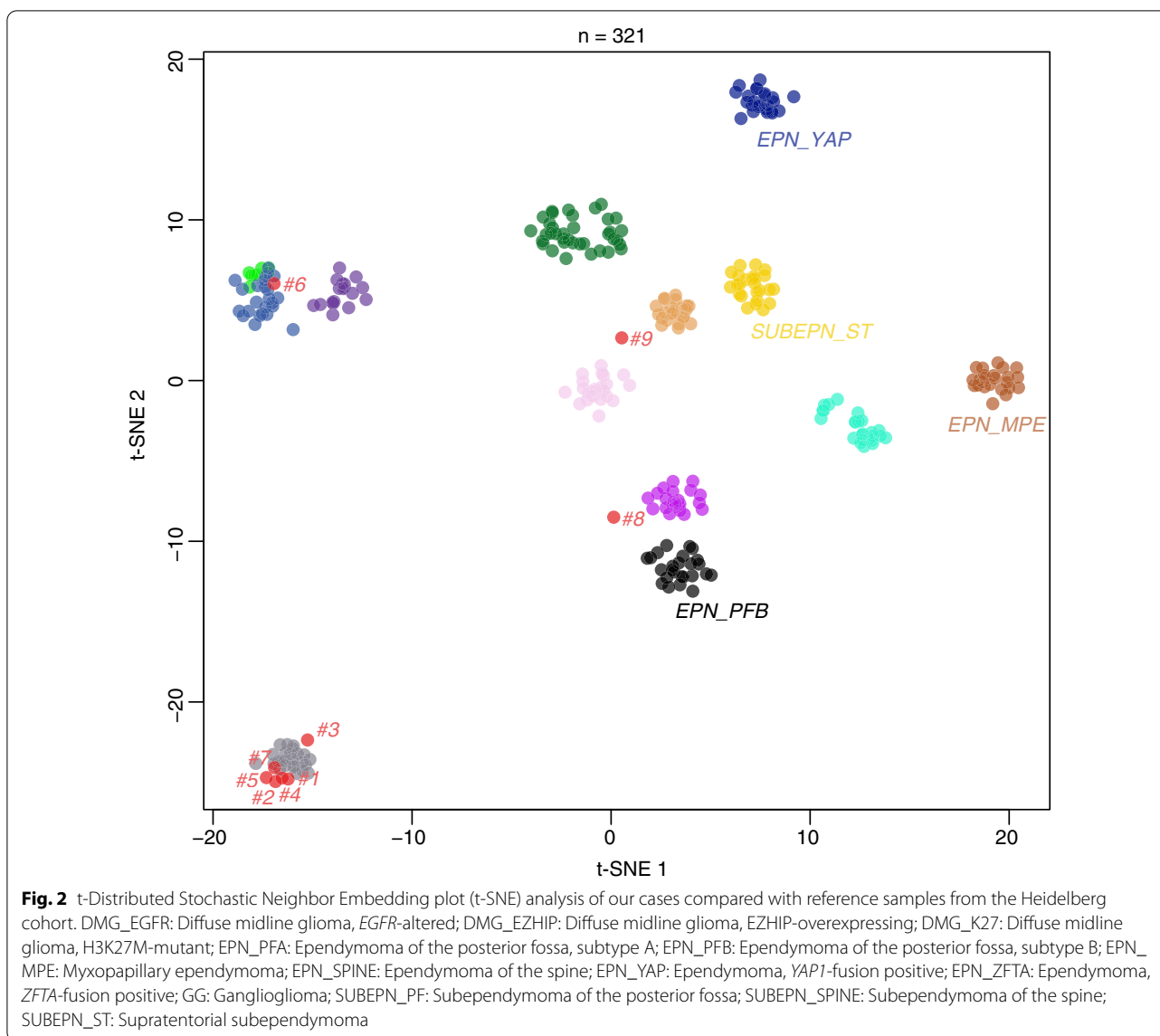
quality of the remaining DNA. At the end of follow-up, 5/6 patients were alive (median follow-up of 68 months) (Table 1).

One case (#8) was classified by the v12.5 of the brain classifier as EPN_PFA, subclass 1a (but with a low calibrated score of 0.45), but the t-SNE analysis did not support this data. The tumor did not cluster within a methylation class, but was in proximity to posterior fossa subependymomas (Fig. 2). This case concerned a 1-year-old boy presenting recent (<1 month) symptoms of intracranial hypertension. The MRI revealed a voluminous and well-circumscribed tumor arising from the right cerebellopontine angle (CPA) with spontaneous hemorrhage and contrast enhancement (Fig. 3a–c). Histopathologically, the tumor presented a solid growth pattern and immunonegativity for Olig2 (Fig. 3d–f). The expression of H3K27M by tumor cells (Fig. 3g) was confirmed by DNA sequencing analysis showing a *HIST1H3B* K27M mutation. This patient died suddenly after 88 months without evidence of relapse or progression, following adjuvant treatments by radiation therapy and chemotherapy. Based on the WHO classification, the integrated diagnosis was EPN_PFA with H3K27M mutation.

Case #6 was classified by the v12.5 of the brain classifier as DMG, H3K27M-mutant, but with a calibrated score of 0.84. This data was confirmed by the t-SNE analysis where it perfectly clustered with DMG, H3 K27-altered, subtype H3 K27-mutant or EZHIP overexpressing (Fig. 2). This case concerned a 7-year-old boy with recent (<3 weeks) symptoms of cranial nerve palsy and hemiparesis revealing a pontine tumor (Fig. 4a, b). Radiologically, the tumor was intrinsic to the pons, infiltrative,

showed a high signal on T2-weighted images, and had focal necrosis with peripheral enhancement (Fig. 4b, c). Diffusion was restricted in one part of the tumor (Fig. 4d, e). Morphologically, this tumor was composed of two distinct glial histopathological components: one solid with ependymal features (pseudorosettes and true rosettes) and a weak expression of Olig2 and one infiltrative component with an Olig2 expression (Fig. 4f–l). Both components expressed H3K27M and an *H3F3A* K27M mutation was confirmed by DNA sequencing analysis (Fig. 4m–n). After the biopsy, the patient received radiation therapy and chemotherapy with Dasatinib, but died 11 months after the initial diagnosis (Additional file 2: Supplementary Table 1). The integrated diagnosis of this case was DMG, H3 K27-altered with ependymal features.

The last case (#9) was classified by the v12.5 of the brain classifier as DMG, H3K27M-mutant (but with a low calibrated score of 0.54), however the t-SNE analysis did not confirm this data. The tumor did not cluster within a methylation class (Fig. 2). This case concerned an 8-year-old boy who did not present a short medical history but headaches and oculomotor nerve palsy lasting nine months before exhibiting rapidly progressing brainstem dysfunction symptoms (trouble swallowing, hemiparesis). The MRI showed a well-circumscribed tumor limited to the *medulla oblongata* with a high T2-weighted signal, without infiltration of the spine (Fig. 5a–c). There was no enhancement after injection of gadolinium (Fig. 5d). There was no restriction of the diffusion (high apparent diffusion coefficient) (Fig. 5e, f). Histopathologically, the tumor was paucicellular with subependymal features and without Olig2 immunopositivity (Fig. 5g, h). However, the tumor showed an infiltrative growth pattern (Fig. 5i).



All tumor cells expressed H3K27M, which was confirmed by DNA sequencing as a K27M *H3F3A* mutation (Fig. 5j). After the biopsy, the patient was treated by radiation therapy and chemotherapy with Everolimus and Bevacizumab, but died eight months after the initial diagnosis (Additional file 2: Supplementary Table 1). Based on the WHO classification and because of discrepancies between histopathology and epigenetic results, no integrated diagnosis was made.

No differences in terms of histopathology and outcome between EPN_PFA EZHIP-overexpressing and their counterpart with H3K27M mutation

After integrated diagnoses, the results of our cohort of confirmed EPN_PFA (n=7) showed that patients

with H3K27M-mutant EPN_PFA (median age of 6 years) were significantly older than EZHIP-overexpressing EPN_PFA patients (median age of 2.4 years) (p = 0.0168) (Fig. 6a), as opposed to DMG patients [4].

Radiologically, EPN_PFA with an H3K27M mutation presented as a well-delineated solid tumor located in the fourth ventricle except for one case located in the cerebellopontine angle (Additional file 1: Supplementary Fig. 2). Peritumoral edema was found in approximately half of cases. Calcifications were present in the 3/3 cases having available CT. By MRI, tumors displayed intense heterogeneous enhancement after gadolinium chelate injection. A lateral extension of the tumors via the foramen of Luschka was present as in EPN_PFA EZHIP-overexpressing whereas their

Table 1 Summary of clinicopathological features of the PFA-EPN, H3K27M-mutant including cases from the literature

	Author Reference	Age (years)/Sex	WHO Grade	Mutation	1q gain/6q loss (CNV)	Methylation class (calibrated score)	Integrated diagnosis	Resection	Adjuvant therapy	Outcome
1	Current study	5/M	ND*	H3T3H3B	Absent/absent	PFA-EPN 1f (0.99)	PFA-EPN	GTR	Radiotherapy	Spinal relapse at 16 months Death at 50 months
2		5/F	ND*	NA	Absent/present	PFA-EPN 1f (0.99)	PFA-EPN	Subtotal resection	Radiotherapy	Spinal relapse at 6 months Alive at 50 months
3		10/F	ND*	H3T3H3C	Absent/absent	PFA-EPN 1a (0.23)	PFA-EPN	GTR	Radiotherapy	Spinal relapse at 107 months Alive at 130 months
4		12/M	ND*	H3T3H3B	Absent/absent	PFA-EPN 1f (0.95)	PFA-EPN	GTR	Radiotherapy	Relapse-free Alive at 101 months
5		9/F	ND*	H3T3H3C	Present/absent	PFA-EPN 1f (0.99)	PFA-EPN	Subtotal resection	Radiotherapy	Relapse at 79 months Alive at 82 months
7		8/M	ND*	H3T3H3D	Absent/absent	PFA-EPN 1f (0.99)	PFA-EPN	GTR	Radiotherapy	Alive at 3 months
8		1.5/M	ND*	H3F3A	Absent/absent	PFA-EPN 1a (0.45)	PFA-EPN	GTR	Radiotherapy Everolimus Avastin	Death at 88 months
10	Gessi [8]	1.5/F	3	H3F3A	NA/NA	PFA-EPN	PFA-EPN	Biopsy	E-HIT 2000 R	Relapse free Alive at 6 months
11		6/F	3	H3T3H3C	NA/NA	PFA-EPN	PFA-EPN	GTR	E-HIT 2000 AB4	Spinal relapse at 19 months Alive at 49 months
12	Nambirajan [13]	2/F	2	H3F3A	Absent/NA	NA	NA	GTR	Radiotherapy	Relapse at 3 months Alive at 24 months
13	Ryall [17]	7/M	3	H3F3A	Absent/absent	NA	NA	GTR	Radiotherapy	Local relapse at 18 months Death at 24 months
14	Tanrikulu [19]	1.5/M	3	NA	NA/NA	NA	NA	GTR	Chemotherapy	Relapse-free Alive at 86 months
15	Yao [21]	2/M	1	H3F3A	NA/NA	NA	NA	No GTR	No	Relapse-free Alive at 60 months
15		43/M	1	H3F3A	NA/NA	NA	NA	No GTR	No	Relapse and death at 37 months
16		13/M	1	H3F3A	NA/NA	NA	NA	No GTR	No	Relapse-free Alive at 40 months
17		20/M	1	H3F3A	NA/NA	NA	NA	No GTR	No	Relapse-free Alive at 3 months

Table 1 (continued)

Author Reference	Age (years)/Sex	WHO Grade	Mutation	1q gain/6q loss (CNV)	Methylation class (calibrated score)	Integrated diagnosis	Resection	Adjuvant therapy	Outcome
Pajtler [15]	NA	NA	<i>HIST1H3B</i> (n = 4) <i>HIST1H3C</i> (n = 7)	NA/NA NA/NA	Ependymoma 1f (9/13) Ependymoma 1a, 1d, 1e	PFA-EPN PFA-EPN	NA NA	NA NA	NA NA
			<i>H3F3A</i> (n = 2)	NA/NA	Ependymoma 1a	PFA-EPN			

CNV: copy number variation; EPN: ependymoma; F: female; GTR: Gross total resection; M: male; NA: not available; ND: not detailed; PFA: posterior fossa group A; WHO: World Health Organization
 * All cases presented high-grade features

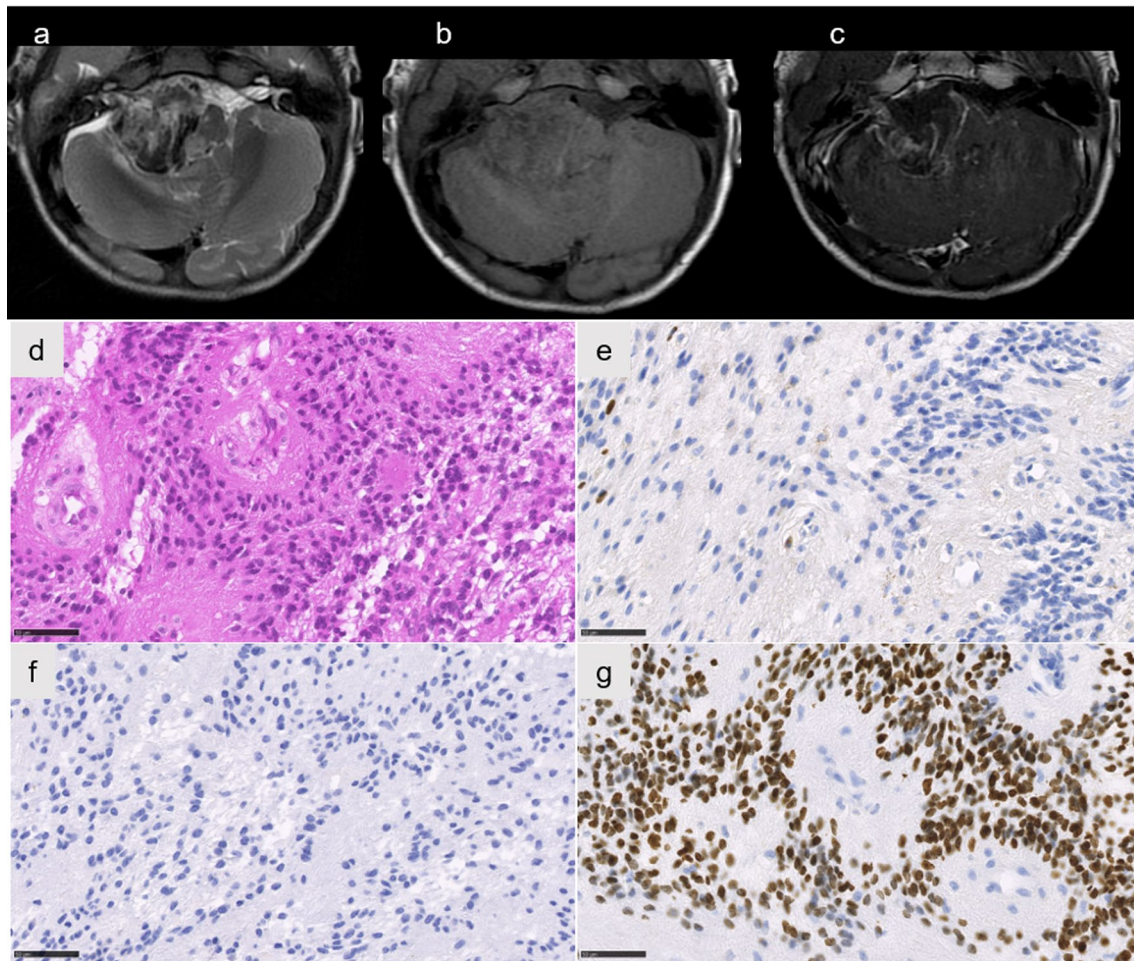


Fig. 3 Radiological and histopathological features of case #8. Axial T2-weighted image showing a circumscribed hemorrhagic lesion of the right cerebellopontine angle (a), with a low signal on T1-weighted images (b), and a peripheral enhancement on T1-weighted image with gadolinium injection (c). Ependymal features with pseudorosettes (d HPS, magnification 400x), associated with no immunoreactivity for Olig2 (e magnification 400x). Neurofilament immunostaining confirming the solid pattern (f magnification 400x). Immunopositivity of H3K27M in all tumor cells (g magnification 400x). Scale bars represent 50 μ m. HPS: Hematoxylin Phloxin Saffron

H3K27M-mutant counterparts did not invade the posterior fossa foramina.

Histopathologically, no differences were found between EPN_PFA EZHIP-overexpressing and EPN_PFA H3K27M-mutant (Additional file 1: Supplementary

Fig. 2). All EPN_PFA H3K27M-mutant showed the histopathological features for EPN, including pseudorosettes and rosettes. All of the tumors were well-circumscribed using neurofilament staining. Calcifications were observed in 5/7 cases which are rare in DMG, H3

(See figure on next page.)

Fig. 4 Radiological and histopathological features of case #6. Sagittal T2-weighted image (a) and FLAIR image (b) showing an infiltrative lesion of the pons with a central liquid part consistent with necrosis, with a peripheral enhancement on T1-weighted image with gadolinium injection (c), and intermediate signal on diffusion-weighted image (d) with partially restricted diffusion on apparent diffusion coefficient map (e). The biopsy highlighted two different histopathological components (f HPS, magnification \times 50). The glial diffuse component (g HPS, magnification 400x), associated with an ependymal component with rosettes (h HPS, magnification 400x). Neurofilament immunostaining confirming the infiltrative pattern in the glial component (i magnification 400x) and a more circumscribed pattern in the ependymal component (j magnification 400x). Diffuse immunopositivity for Olig2 in the glial component (k magnification \times 400), and partial expression of Olig2 in the ependymal component (l magnification \times 400). Diffuse immunopositivity of H3K27M in both tumoral components (m–n magnification 400x). Scale bars represent 1 mm (f) and 50 μ m (g–n). HPS: Hematoxylin Phloxin Saffron

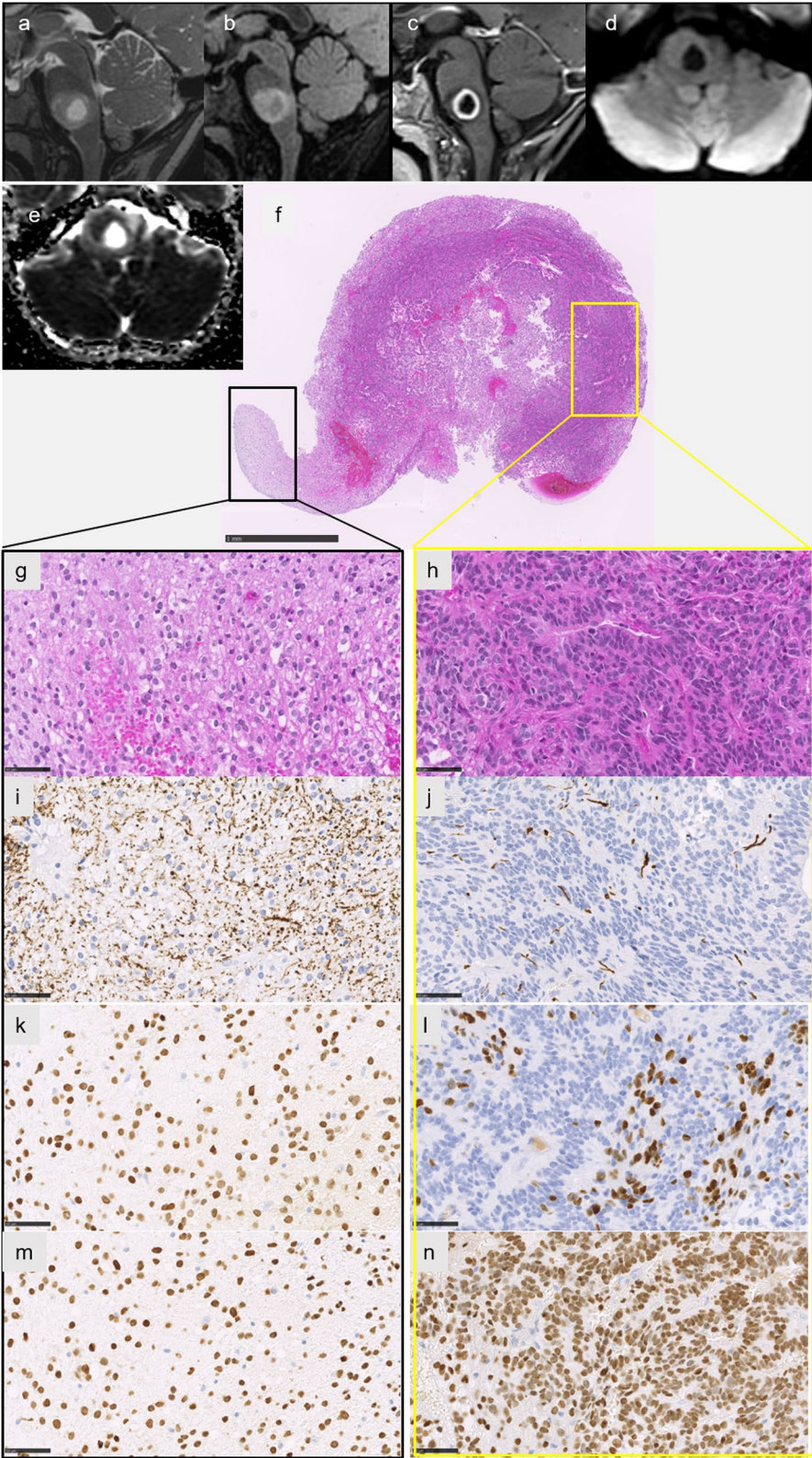


Fig. 4 (See legend on previous page.)

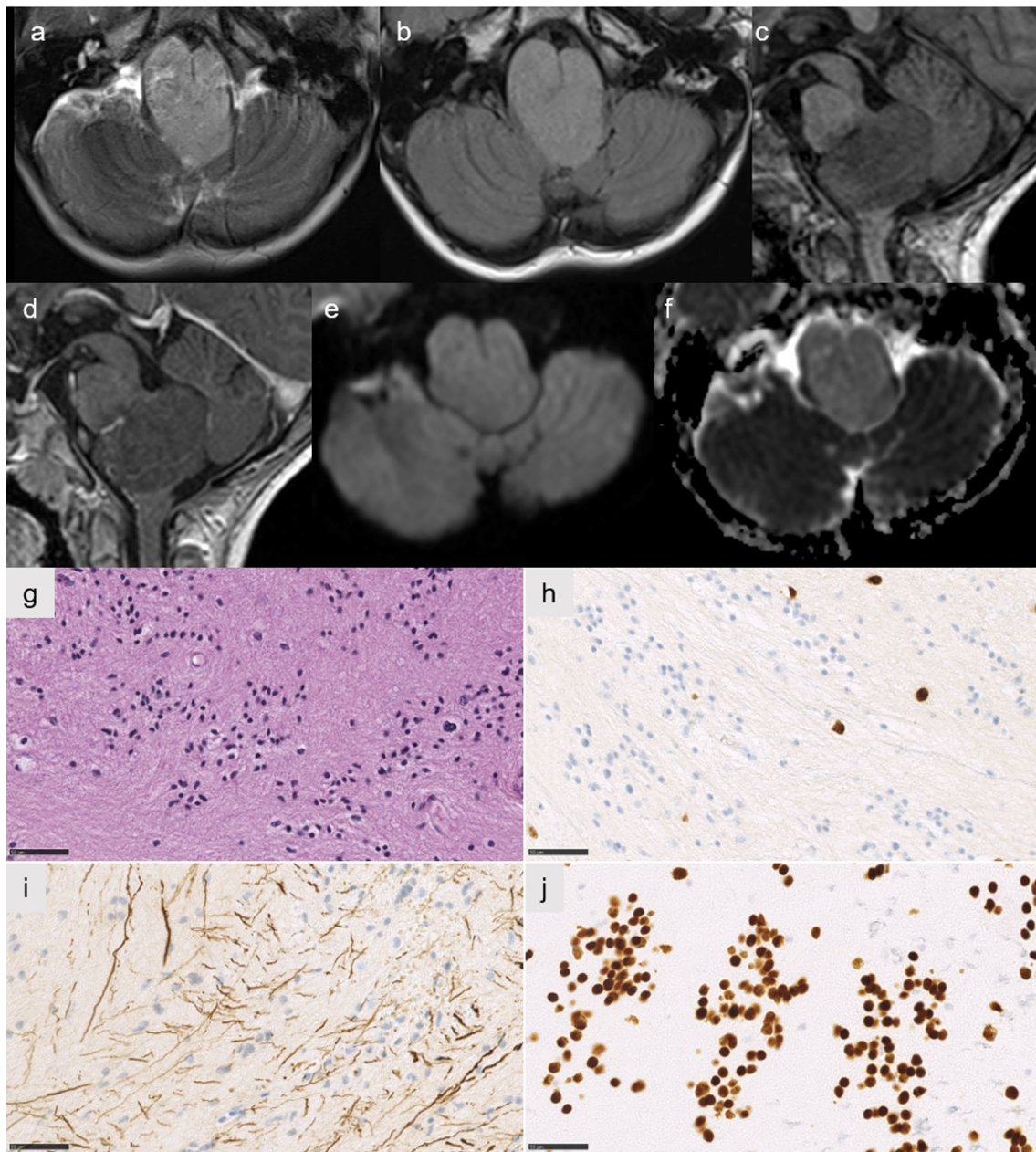
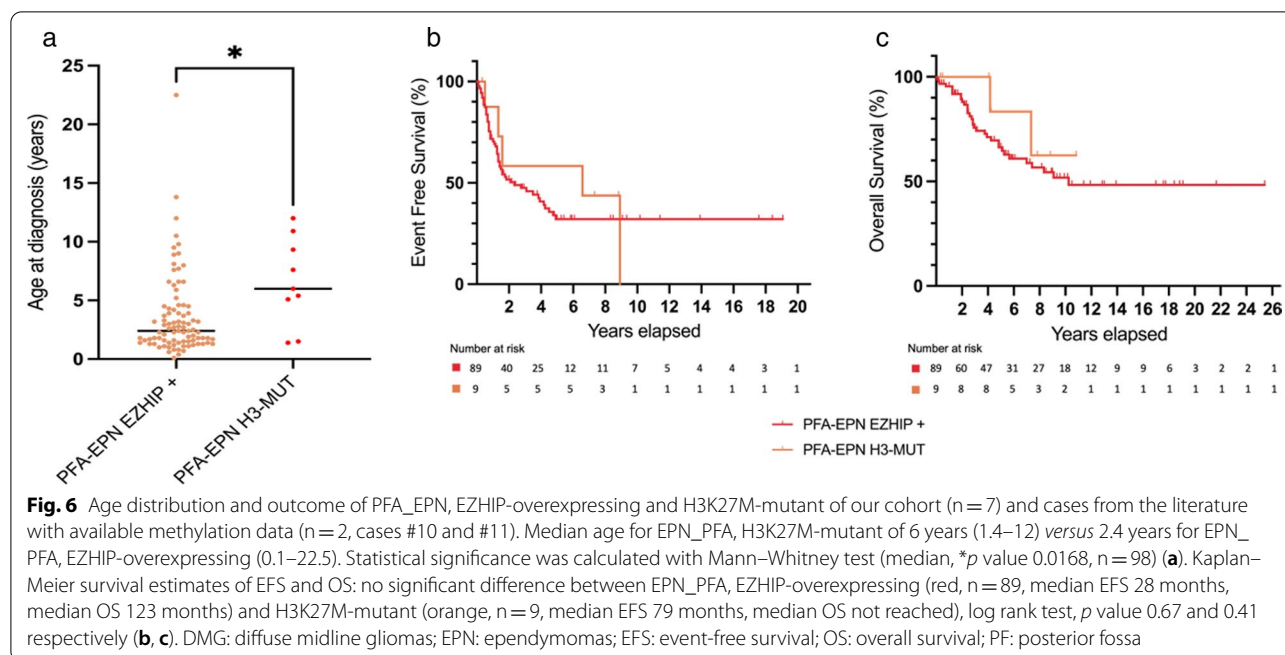


Fig. 5 Radiological and histopathological features of case #9. Axial T2-weighted and FLAIR image showing a circumscribed lesion of the *medulla oblongata* (a,b), without enhancement on sagittal T1-weighted image with gadolinium injection (c before injection, d after injection), and low signal on diffusion weighted image (e) with increased diffusion on apparent diffusion coefficient map (f). A paucicellular tumor with subependymal features (g HPS, magnification 400x). No immunoreactivity for Olig2 except in residual glial cells (h HPS, magnification 400x). Neurofilament immunostaining showing an infiltrative pattern (i magnification 400x). Diffuse immunopositivity of H3K27M in tumor cells (j magnification 400x). Scale bars represent 50 μ m. HPS: Hematoxylin Phloxin Saffron

K27-altered. High-grade features, including prominent mitotic activity (7/7 cases), necrosis (5/7 cases) and microvascular proliferation (5/7 cases) were present. Immunohistochemical analyses showed classical features of EPN with a diffuse expression of GFAP, a focal or

absent expression of Olig2 and dot-like immunopositivity for EMA in all cases.

Overall survival (OS) and event-free survival (EFS) of EZHIP-overexpressing compared to H3K27M-mutant EPN_PFA seem to present no statistical difference



(Fig. 6b, c). To note, the case classified as DMG with ependymal features, H3K27M-mutant (case #6) presented an OS similar to DMG, rather than EPN.

Discussion

This series constitutes the first attempt to perform a comprehensive clinico-radiological, histopathological, genetic and epigenetic characterization of EPN_PFA H3 K27M-mutant. Our cohort highlights the difficulties encountered when reaching this diagnosis and the potential overlaps with DMG, H3 K27-altered. The DNA-methylation profiling showed that H3 K27M-mutant posterior fossa tumors with ependymal/subependymal features may represent different epigenetic subgroups, confirming that the DNA-methylation profile is not dominated by consequences of H3 mutations but possibly by the cell of origin. Our results confirm that DMG, H3 K27-altered, may present morphological ependymal features [18]. These results reinforce the essential criteria of the WHO classification of tumors of the CNS for DMG, H3 K27-altered [11, 12]. However, our results indicate that diagnostic criteria of EPN_PFA and DMG, H3 K27-altered do not permit the classification of all posterior fossa tumors H3K27M-mutant. Indeed, one of our cases (#9) was not classified using the DNA-methylation profile. Further cases are needed to better characterize and clarify these difficult cases having overlapping similarities to EPN, subependymomas and DMG. Because most reported cases lack DNA-methylation profiles and the main histopathological criteria (such as the growth pattern and

Olig2 expression), the literature review remains difficult to analyze but the hypothesis of a DMG with ependymal/subependymal features could be proposed [2, 13, 17, 19, 21]. Indeed, contrary to DMG, H3 K27-altered, H3F3A mutations do not represent the main molecular event in EPN_PFA, H3K27M-mutant, in which H3.1 gene mutations are overrepresented [6]. Our results compiled with those from the literature (including only articles with DNA-methylation analyses) show that H3.1 gene K27M mutations represent 85% of mutations (17/20 cases) encountered in EPN_PFA including: *HIST1H3C* (n = 10), *HIST1H3B* (n = 6), and herein, for the first time (including in the DMG population), *HIST1H3D* (n = 1) [8, 15]. The three remaining cases (15%) harbored an *H3F3A* K27M mutation [8, 15]. After integrated diagnoses, the frequency of H3K27M mutations in EPN_PFA of our cohort (7/116, 6%) is slightly higher than previous series (1 to 4% among the cohorts) [13, 15, 17]. Our results suggest that this PFA subgroup may differ from its overexpressing EZHIP counterpart, in terms of age and location. All but one tumor (located in the cerebellopontine angle) were midline and located in the fourth ventricle, which is less frequently observed in EPN_PFA with EZHIP-overexpression [1]. A histopathological central review of our cases and the literature showed that H3K27M-mutant EPN_PFA were similar to their counterparts with an EZHIP overexpression [8, 15]. We confirmed that EPN_PFA H3K27M-mutant are mainly classified within the subgroup 1f using DNA-methylation profiling, as previously reported [15].

In summary, H3K27M-mutant EPN_PFA may be a challenging diagnosis considering the pitfall of DMG with ependymal features, having important therapeutic and care support consequences. Tumor location, diffuse *versus* circumscribed tumoral architecture, Olig2 expression, type of histone gene mutations and DNA-methylation profiling must be considered in the integrated diagnosis.

Supplementary Information

The online version contains supplementary material available at <https://doi.org/10.1186/s40478-022-01442-4>.

Additional file 1: Figure 1. Copy number profiles of cases of the cohort.

Additional file 2: Table 1. Summary of clinicopathological features of the H3K27M-mutant diffuse midline gliomas with ependymal tumor patients of the current study.

Acknowledgements

We would like to thank the laboratory technicians at the GHU Paris Neuro Sainte-Anne for their assistance, as well as the Integragen platform for their technical collaboration on the DNA-methylation analyses. We would like to thank Philipp Sievers from Heidelberg for performing the t-SNE analysis.

Funding

JG received funding from the charity "l'Etoile de Martin" and from the Carrefour Foundation "Les Boucles du Cœur" for the sequencing programme RARE.

Declarations

Competing interests

The authors declare that they have no conflict of interest.

Author details

¹Department of Pediatric Oncology, Gustave Roussy, Université Paris-Saclay, 94805 Villejuif, France. ²U981, Molecular Predictors and New Targets in Oncology, INSERM, Gustave Roussy, Université Paris-Saclay, 94805 Villejuif, France. ³Department of Biochemistry and Oncogenetic, Paul Brousse Hospital, 94804 Villejuif, France. ⁴Pediatric Radiology Department, Hôpital Necker Enfants Malades, AP-HP, Paris, France. ⁵Université Paris Cité, UMR 1163, Institut Imagine and INSERM U1299, Paris, France. ⁶Department of Pathology, Ponchaillou Hospital, Rennes, France. ⁷Department of Oncology, Ponchaillou Hospital, Rennes, France. ⁸Department of Pediatric Neurosurgery, Necker Hospital, APHP, Université Paris Descartes, Sorbonne Paris Cité, 75015 Paris, France. ⁹Department of Neuropathology, GHU Paris-Psychiatrie Et Neurosciences, Sainte-Anne Hospital, 1, rue Cabanis, 75014 Paris, France. ¹⁰Inserm, UMR 1266, IMA-Brain, Institut de Psychiatrie Et Neurosciences de Paris, Paris, France.

Received: 26 July 2022 Accepted: 1 September 2022

Published online: 14 September 2022

References

- AlRayahi J, Zapotocky M, Ramaswamy V, Hanagandi P, Branson H, Mubarak W, Raybaud C, Laughlin S (2018) Pediatric brain tumor genetics: what radiologists need to know. *Radiographics* 38:2102–2122. <https://doi.org/10.1148/rg.2018180109>
- Alturkustani M, Cotter JA, Mahabir R, Hawes D, Koschmann C, Venneti S, Judkins AR, Szymanski LJ (2021) Autopsy findings of previously described case of diffuse intrinsic pontine glioma-like tumor with EZHIP expression and molecular features of PFA ependymoma. *Acta Neuropathol Commun* 9:113. <https://doi.org/10.1186/s40478-021-01215-5>
- Bugiani M, van Zanten SEMV, Caretti V, Schellen P, Aronica E, Noske DP, Vandertop WP, Kaspers GJL, van Vuurden DG, Wesseling P, Hulleman E (2017) Deceptive morphologic and epigenetic heterogeneity in diffuse intrinsic pontine glioma. *Oncotarget* 8:60447–60452. <https://doi.org/10.18632/oncotarget.19726>
- Capper D, Jones DTW, Sill M, Hovestadt V, Schrimpf D, Sturm D, Koelsche C, Sahm F, Chavez L, Reuss DE, Kratz A, Wefers AK, Huang K, Pajtler KW, Schweizer L, Stichel D, Olar A, Engel NW, Lindenberg K, Harter PN, Braczynski A, Plate KH, Dohmen H, Garvalov BK, Coras R, Hölsken A, Hewer E, Bewerunge-Hudler M, Schick M, Fischer R, Beschoner R, Schittenhelm J, Staszewski O, Wani K, Varlet P, Pages M, Temming P, Lohmann D, Selt F, Witt H, Milde T, Witt O, Aronica E, Giangaspero F, Rushing E, Scheurlen W, Geisenberger C, Rodriguez FJ, Becker A, Preusser M, Haberler C, Bjerkvig R, Cryan J, Farrell M, Deckert M, Hench J, Frank S, Serrano J, Kannan K, Tsirogos A, Brück W, Hofer S, Brehmer S, Seiz-Rosenhagen M, Hänggi D, Hans V, Roznoki S, Hansford JR, Kohlhof P, Kristensen BW, Lechner M, Lopes B, Mawrin C, Ketter R, Kulozik A, Khatib Z, Heppner F, Koch A, Jouvett A, Keohane C, Mühleisen H, Mueller W, Pohl U, Prinz M, Bennis A, Zapotka M, Gottardo NG, Driever PH, Kramm CM, Müller HL, Rutkowski S, von Hoff K, Frühwald MC, Gnekow A, Fleischhack G, Tippelt S, Calaminus G, Monoranu C-M, Perry A, Jones C, Jacques TS, Radlwimmer B, Gessi M, Pietsch T, Schramm J, Schackert G, Westphal M, Reifenberger G, Wesseling P, Weller M, Collins VP, Blümcke I, Bendszus M, Debus J, Huang A, Jabado N, Northcott PA, Paulus W, Gajjar A, Robinson G, Taylor MD, Jaunmuktane Z, Ryzhova M, Platten M, Unterberg A, Wick W, Karajannis MA, Mittelbronn M, Acker T, Hartmann C, Aldape K, Schüller U, Buslei R, Lichter P, Kool M, Herold-Mende C, Ellison DW, Hasselblatt M, Snuderl M, Brandner S, Korshunov A, von Deimling A, Pfister SM (2018) DNA methylation-based classification of central nervous system tumours. *Nature* 555:469–474. <https://doi.org/10.1038/nature26000>
- Castel D, Kergerohen T, Tauziède-Espariat A, Mackay A, Ghermaoui S, Lechapt E, Pfister SM, Kramm CM, Boddaert N, Blauwblomme T, Puget S, Beccaria K, Jones C, Jones DTW, Varlet P, Grill J, Debily M-A (2020) Histone H3 wild-type DIPG/DMG overexpressing EZHIP extend the spectrum diffuse midline gliomas with PRC2 inhibition beyond H3–K27M mutation. *Acta Neuropathol (Berl)* 139:1109–1113. <https://doi.org/10.1007/s00401-020-02142-w>
- Castel D, Philippe C, Calmon R, Le Dret L, Truffaux N, Boddaert N, Pagès M, Taylor KR, Saulnier P, Lacroix L, Mackay A, Jones C, Sainte-Rose C, Blauwblomme T, Andreiulo F, Puget S, Grill J, Varlet P, Debily M-A (2015) Histone H3F3A and HIST1H3B K27M mutations define two subgroups of diffuse intrinsic pontine gliomas with different prognosis and phenotypes. *Acta Neuropathol (Berl)* 130:815–827. <https://doi.org/10.1007/s00401-015-1478-0>
- Dottermusch M, Uksul N, Knappe UJ, Erdlenbruch B, Wefers AK (2022) An H3F3A K27M-mutation in a sonic hedgehog medulloblastoma. *Brain Pathol Zurich Switz* 32:e13024. <https://doi.org/10.1111/bpa.13024>
- Gessi M, Capper D, Sahm F, Huang K, von Deimling A, Tippelt S, Fleischhack G, Scherbaum D, Alfer J, Juhnke B-O, von Hoff K, Rutkowski S, Warmuth-Metz M, Chavez L, Pfister SM, Pietsch T, Jones DTW, Sturm D (2016) Evidence of H3 K27M mutations in posterior fossa ependymomas. *Acta Neuropathol (Berl)* 132:635–637. <https://doi.org/10.1007/s00401-016-1608-3>
- Joyon N, Tauziède-Espariat A, Alentorn A, Giry M, Castel D, Capelle L, Zanella M, Varlet P, Bielle F (2017) K27M mutation in H3F3A in ganglioglioma grade I with spontaneous malignant transformation extends the histopathological spectrum of the histone H3 oncogenic pathway. *Neuropathol Appl Neurobiol* 43:271–276. <https://doi.org/10.1111/nan.12329>
- Kleinschmidt-DeMasters BK, Donson A, Foreman NK, Dorris K (2017) H3 K27M mutation in Gangliogliomas can be Associated with poor prognosis. *Brain Pathol Zurich Switz* 27:846–850. <https://doi.org/10.1111/bpa.12455>
- Louis DN, Giannini C, Capper D, Paulus W, Figarella-Branger D, Lopes MB, Batchelor TT, Cairncross JG, van den Bent M, Wick W, Wesseling P (2018) cIMPACT-NOW update 2: diagnostic clarifications for diffuse midline glioma, H3 K27M-mutant and diffuse astrocytoma/anaplastic astrocytoma, IDH-mutant. *Acta Neuropathol (Berl)* 135:639–642. <https://doi.org/10.1007/s00401-018-1826-y>
- Louis DN, Perry A, Wesseling P, Brat DJ, Cree IA, Figarella-Branger D, Hawkins C, Ng HK, Pfister SM, Reifenberger G, Soffietti R, von Deimling A, Ellison DW (2021) The 2021 WHO Classification of Tumors of the Central

- Nervous System: a summary. *Neuro-Oncol* noab106. <https://doi.org/10.1093/neuonc/noab106>
13. Nambirajan A, Sharma A, Rajeshwari M, Boorgula MT, Doddamani R, Garg A, Suri V, Sarkar C, Sharma M (2020) EZH2 inhibitory protein (EZHIP/Cxor67) expression correlates strongly with H3K27me3 loss in posterior fossa ependymomas and is mutually exclusive with H3K27M mutations. *Brain Tumor Pathol*. <https://doi.org/10.1007/s10014-020-00385-9>
 14. Pagès M, Beccaria K, Boddaert N, Saffroy R, Besnard A, Castel D, Fina F, Baretts D, Barret E, Lacroix L, Bielle F, Andreiuolo F, Tauziède-Espariat A, Figarella-Branger D, Puget S, Grill J, Chrétien F, Varlet P (2016) Co-occurrence of histone H3 K27M and BRAF V600E mutations in paediatric midline grade I ganglioglioma. *Brain Pathol Zurich Switz*. <https://doi.org/10.1111/bpa.12473>
 15. Pajtler KW, Wen J, Sill M, Lin T, Orisme W, Tang B, Hübner J-M, Ramaswamy V, Jia S, Dalton JD, Hauptfear K, Rogers HA, Punchihewa C, Lee R, Easton J, Wu G, Ritzmann TA, Chapman R, Chavez L, Boop FA, Klimo P, Sabin ND, Ogg R, Mack SC, Freibaum BD, Kim HJ, Witt H, Jones DTW, Vo B, Gajjar A, Pounds S, Onar-Thomas A, Roussel MF, Zhang J, Taylor JP, Merchant TE, Grundy R, Tatevossian RG, Taylor MD, Pfister SM, Korshunov A, Kool M, Ellison DW (2018) Molecular heterogeneity and Cxor67 alterations in posterior fossa group A (PFA) ependymomas. *Acta Neuropathol (Berl)* 136:211–226. <https://doi.org/10.1007/s00401-018-1877-0>
 16. Pratt D, Quezado M, Abdullaev Z, Hawes D, Yang F, Garton HJL, Judkins AR, Mody R, Chinnaiyan A, Aldape K, Koschmann C, Venneti S (2020) Diffuse intrinsic pontine glioma-like tumor with EZHIP expression and molecular features of PFA ependymoma. *Acta Neuropathol Commun* 8:37. <https://doi.org/10.1186/s40478-020-00905-w>
 17. Ryall S, Guzman M, Elbabaa SK, Luu B, Mack SC, Zapotocky M, Taylor MD, Hawkins C, Ramaswamy V (2017) H3 K27M mutations are extremely rare in posterior fossa group A ependymoma. *Childs Nerv Syst ChNS Off J Int Soc Pediatr Neurosurg* 33:1047–1051. <https://doi.org/10.1007/s00381-017-3481-3>
 18. Solomon DA, Wood MD, Tihan T, Bollen AW, Gupta N, Phillips JJJ, Perry A (2016) Diffuse midline gliomas with histone H3–K27M mutation: a Series of 47 Cases Assessing the Spectrum of Morphologic Variation and Associated Genetic Alterations. *Brain Pathol Zurich Switz* 26:569–580. <https://doi.org/10.1111/bpa.12336>
 19. Tanrikulu B, Danyeli AE, Özek MM (2020) Is H3K27me3 status really a strong prognostic indicator for pediatric posterior fossa ependymomas? A single surgeon, single center experience. *Childs Nerv Syst ChNS Off J Int Soc Pediatr Neurosurg* 36:941–949. <https://doi.org/10.1007/s00381-020-04518-5>
 20. Wang L, Lu D, Piao Y (2022) A 2-year-old girl with posterior fossa mass. *Brain Pathol Zurich Switz* 32:e13026. <https://doi.org/10.1111/bpa.13026>
 21. Yao K, Duan Z, Wang Y, Zhang M, Fan T, Wu B, Qi X (2019) Detection of H3K27M mutation in cases of brain stem subependymoma. *Hum Pathol* 84:262–269. <https://doi.org/10.1016/j.humpath.2018.10.011>

Publisher's Note

Springer Nature remains neutral with regard to jurisdictional claims in published maps and institutional affiliations.

Ready to submit your research? Choose BMC and benefit from:

- fast, convenient online submission
- thorough peer review by experienced researchers in your field
- rapid publication on acceptance
- support for research data, including large and complex data types
- gold Open Access which fosters wider collaboration and increased citations
- maximum visibility for your research: over 100M website views per year

At BMC, research is always in progress.

Learn more biomedcentral.com/submissions

